

Molecularly Organized Langmuir–Blodgett Films from a Ruthenium Biphosphine Complex

K. Wohnrath,^{*,†} C. J. L. Constantino,[‡] P. A. Antunes,[‡] P. M. dos Santos,[†] A. A. Batista,[§]
R. F. Aroca,[⊥] and O. N. Oliveira, Jr.[#]

Departamento de Química, UEPG, Ponta Grossa/PR, Brazil; Departamento de Física, Química e Biologia, FCT/UNESP, Presidente Prudente/SP, Brazil; Departamento de Química, UFSCar, São Carlos/SP, Brazil; Materials and Surface Science Group, School of Physical Sciences, University of Windsor, Windsor, Ontario, Canada N9B 3P4; and Universidade de São Paulo, Instituto de Física de São Carlos, São Carlos/SP, Brazil

Received: March 9, 2004; In Final Form: January 14, 2005

Langmuir–Blodgett (LB) films from a ruthenium complex *mer*-[RuCl₃(dppb)(4-Mepy)] (dppb = PPh₂(CH₂)₄-PPh₂; 4-Mepy = 4-methylpyridine), termed Ru-Pic, display a distinct color, which is different from the coloration exhibited by cast films or chloroform solutions. The solution and cast films are red, while the LB films are green-bluish. The manifestation of the blue color in the LB film finds its explanation in a unique absorption band at 690 nm, which is associated with the oxidation of the phosphine moieties. Fluorescence emission and absorption–reflection infrared spectroscopy measurements revealed the molecular organization in the LB films. In contrast, cast films showed a random distribution of complexes. Surface-enhanced Raman scattering was also used in an attempt to identify the main interactions in Ru-Pic.

Introduction

We are investigating the Langmuir film-forming ability of biphosphine ruthenium complexes to produce Langmuir–Blodgett (LB) films.^{1,2} Such films may find applications in heterogeneous catalysis,^{3,4} in chemical and biological sensors,⁵ and also in modified electrodes for electrocatalysis.^{6–8} The present work complements our previous efforts to obtain a redox center that retains the Ru(dioxolene)₂ unit in the monolayers using phosphine ligands with long alkyl chains coordinated to the Ru center. Initial efforts were unsuccessful for amphiphilic ruthenium(II) compounds containing long aliphatic chains due to the instability arising from hydrolysis of the ester groups.^{9,10} The problem was solved in 1993,¹¹ when it was realized that the complex [Ru(P(C₁₈H₃₇)₃)(DTBSq)] (DTBSq = 3,5-di-*tert*-butyl-*o*-benzosemiquinonate) can form organized monolayer at the air/water interface, which can then be transferred onto a hydrophobic surface. In a parallel work,¹² films were produced from mixtures of stearic acid and a ruthenium complex with no alkyl chain substituent, [Ru(dppen)₃]²⁺ (dppen = 4,7-diphenyl-1,10-phenanthroline), where an ionic-pair interaction occurred between the two components. Such a mixed monolayer approach was also employed for other biphosphinic compounds, e.g., [Ru(dppe)(4'-totpy)(H₂O)]ClO₄, where dppe = PPh₂(CH₂)₂-PPh₂ and 4'-totpy = 4'-(4-tolyl-2,2':6',2''-terpyridine).¹³ For the latter, Fourier transform infrared absorption (FTIR) characterization confirmed that the acid molecules were ionized and complexed with the ruthenium complex molecules. Recent reports¹⁴ have also shown that metal–ruthenium complexes exhibiting a higher or lesser amphiphilic character can form stable monolayers on water. Here, we discuss the Langmuir and

LB films of a semiamphiphilic ruthenium complex *mer*-[RuCl₃(dppb)(4-Mepy)] (dppb = PPh₂(CH₂)₄-PPh₂; 4-Mepy = 4-methylpyridine).¹⁵ The molecular organization was extracted from the information provided by surface pressure–molecular area (π – A) isotherms, atomic force microscopy (AFM), UV–vis absorption, FTIR, reflection–absorption infrared spectroscopy (RAIRS), Raman scattering, and fluorescence.

Experimental Section

The complex *mer*-[RuCl₃(dppb)(4-Mepy)], Ru-Pic, was prepared according to ref 15; its structure is shown in Figure 1. Langmuir monolayers were spread from chloroform (Merck) solutions on aqueous subphases, with ultrapure water supplied by a Millipore system with resistivity of 18.2 M Ω cm, in a KSV5000 Langmuir trough. Surface pressure was measured using a Wilhelmy plate. The trough is installed in a class 10 000 clean room. The Langmuir monolayers were spread at room temperature of 20 °C, with 15 min elapsing before compression for solvent evaporation. The speed of barrier compression was 10 mm min^{−1}, and monolayer stability was investigated by monitoring the area change at a fixed pressure (16 mN m^{−1}) for ca. 10 min until the monolayer was stable, which was denoted by no change in area per molecule.

The monolayers were transferred as Y-type LB films onto different substrates depending on the characterization technique, viz. quartz for UV–vis spectroscopy, ITO (Asahi Glass Co.) for AFM, Si substrates (2 mm thick, diameter 13 mm, from Aldrich) for FTIR. For surface-enhanced (resonance) Raman scattering (SE(R)RS) and RAIRS, glass covered with 10 and 100 nm mass thickness of evaporated Ag films were used as substrates, respectively. Ag evaporation was performed with the glass kept at 100 °C and under a 10^{−6} Torr atmosphere. In the LB film fabrication the dipping speed was 3 mm min^{−1} for the withdrawal as well as immersion of the substrate, with a waiting time of 5 min when the substrate was out of the water, before the next layer was transferred. Transfer ratios were typically

[†] UEPG.

[‡] FCT/UNESP.

[§] UFSCar.

[⊥] University of Windsor.

[#] Universidade de São Paulo.

* To whom correspondence should be addressed: Tel +55-42-220-3731, Fax +55-42-220-3042; e-mail kawoh@uepg.br.

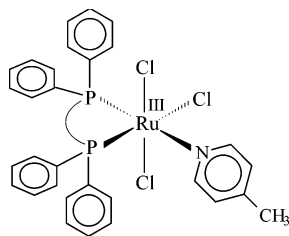


Figure 1. Structure of the complex *mer*-[RuCl₃(dppb)(4-Mepy)], Ru-Pic.

0.9 for downstrokes and 1.2 for upstrokes. FTIR spectra were obtained on LB films deposited onto Si wafers, using a Bomem Michelson FT, model MB 102. The electronic absorption spectra for LB and cast films and solution were recorded in a Hitachi U-3000 spectrophotometer.

Raman (Stokes) and emission spectra were recorded at room temperature (20 °C) with a Renishaw Research Raman microscope system RM2000 equipped with a computer-controlled 3-axis encoded (XYZ) motorized stage with a minimum step of 0.1 μm , a Leica microscope (DMLM series), and a Peltier cooled (−70 °C) CCD array detector. The spectrograph is equipped with a 1200 g/mm grating. The Raman and emission spectra were recorded with ca. 4 cm^{-1} resolution using the Leica microscope with 50 \times microscope objective to focus the laser beam onto a spot of ca. 1.0 μm^2 . The high throughput of the instrument permits the use of very low power lasers at the sample such as ca. 450 μW for the 633 nm and ca. 125 μW for the 514.5 nm laser lines. Data acquisition and analysis were carried out using the WiRE software for Windows and Galactic Industries GRAMS/32 C software including the 3D package. To check the molecular organization in the LB film, transmission for LB films on Si and bulk (powder dispersed in KBr pellet) and RAIRS for the LB film on Ag mirror were recorded at the mid-infrared using a Bomem DA3 Fourier transform infrared spectrometer equipped with a MCT detector. Other experimental conditions were 1024 scans, resolutions of 1 cm^{-1} for the bulk and 4 cm^{-1} for the LB films, and the sample chamber was evacuated until 0.8 Torr. The RAIRS measurements were recorded at an incident angle of 80°. The electronic absorption spectra for the bulk sample were carried out with a Varian UV-vis spectrophotometer model Cary 50.

Results and Discussion

Monolayers at the Liquid–Air Interface. The π - A isotherm of Ru-Pic seen in Figure 2 shows a phase transition at ca. 38 \AA^2 . The area per molecule at high surface pressures, obtained by extrapolation at the condensed state to zero surface pressure, is ca. 25 \AA^2 . The area per molecule is much smaller than the value expected for the Ru-Pic molecule, particularly when the ring lies parallel to the water surface. In fact, the theoretical calculation, using the CPK model in Hyperchem, for the Ru-Pic molecule is estimated to be ca. 148 \AA^2 . There are two possible explanations for such a large difference in the area per molecule: the first is that Ru-Pic molecules are oriented perpendicularly to the subphase, leading to very small values of area per molecule. The second alternative is the formation of multilayer stacks at the air/water interface.^{16,17} In fact, successive compression–expansion cycles of the Ru-Pic Langmuir film resulted in lower areas per molecule, which could be due to either loss of material to the subphase or molecular reorganization leading to nonmonomolecular structures. Since stabilization is reached after three cycles, the decrease in area during the previous cycles is probably due to the formation of nonmonomolecular structures.

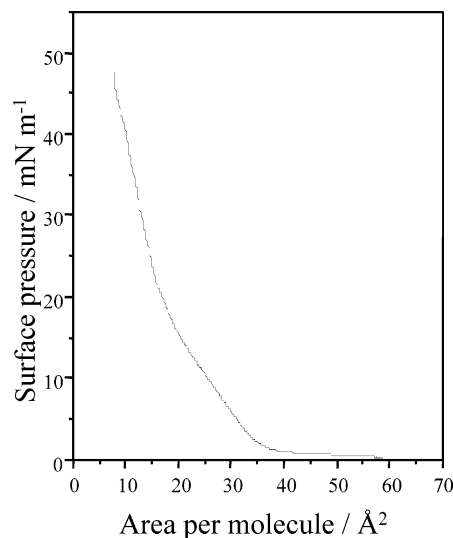


Figure 2. Pressure–area isotherm for a Ru-Pic film on ultrapure water subphase.

Langmuir–Blodgett (LB) Films. Figure 3a shows the UV-vis spectra for neat Ru-Pic complex in solution, for the solid as powder, for a cast film, and for an LB film. For the first three cases, where a random molecular orientation can be safely assumed, the spectra are quite similar. The absorption spectrum of the LB film is clearly different. The main absorption band of the Ru-Pic in solution has a maximum at 530 nm. Absorptions can also be seen at 350 and 450 nm. The band at 350 nm can be tentatively assigned to the ligand–metal charge-transfer transition (LMTC), which corresponds to the electron transfer from the orbitals ($3p\sigma^*\text{d}\pi$) of the phosphorus atom of the biphosphinic ligands dppb to the orbital $d\pi$ of the metal. The band at 450 nm can be associated with the electron transfer from the nitrogen atom to the metal. The main band at 530 nm could be related to the transition from the chlorine orbitals to the metal [$p\pi(\text{Cl}) \rightarrow d\pi(\text{Ru(III)})$].¹⁷ However, for the LB film, a totally different absorption spectrum is observed, and this deviation needs further discussion.

The Ru-Pic LB film thickness increases linearly with the number of layers transferred to the solid substrate as can be seen in Figure 3b, where the absorbance at 520 nm is plotted against the number of deposited layers. However, AFM images showed that the Ru-Pic LB films are not homogeneous, showing defects and aggregates.¹⁸ Nevertheless, the UV-vis absorption of a Ru-Pic LB film composed of 51 monolayers is within the straight line. The spectrum shows an electronic absorption band centered at 690 nm. The latter can be visually detected due to bluish-green color of the LB film, in contrast with the red solution and cast films. The change in the absorption spectrum could be associated with the order induced by the LB technique. However, it is also possible that the electronic absorption effect may result from the interaction of Ru-Pic with water molecules during film fabrication. To distinguish between these two possibilities, a sample in which Ru-Pic molecules were in contact with water was prepared. A chloroform solution of Ru-Pic was spread onto a flask containing pure water at room temperature. After 24 h, a green precipitate was collected by filtration, washed with Et_2O , and dried under vacuum. The FTIR spectrum for this sample is shown in Figure 4, to be compared with the spectrum for Ru-Pic dispersed in a KBr pellet (no interaction with water). The presence in Figure 4 of an additional band at 1187 cm^{-1} , assigned to the P–O bond,¹⁹ in the Ru-Pic sample that had been in contact with water indicates oxidation

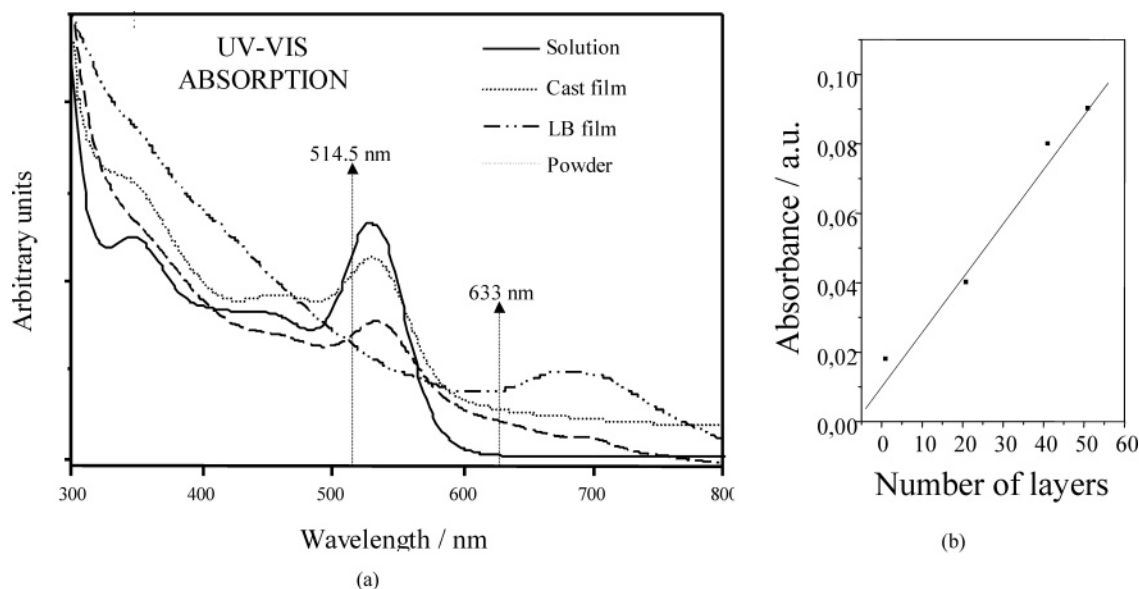


Figure 3. (a) Absorption spectra of Ru-Pic: (—) in CHCl_3 solution, (\cdots) cast film, ($- \cdot -$) powder of Ru-Pic, ($- \cdot \cdot -$) LB film transferred from pure water subphase. All films were deposited onto ITO. (b) Absorbance at 520 nm vs number of deposited Ru-Pic LB layers.

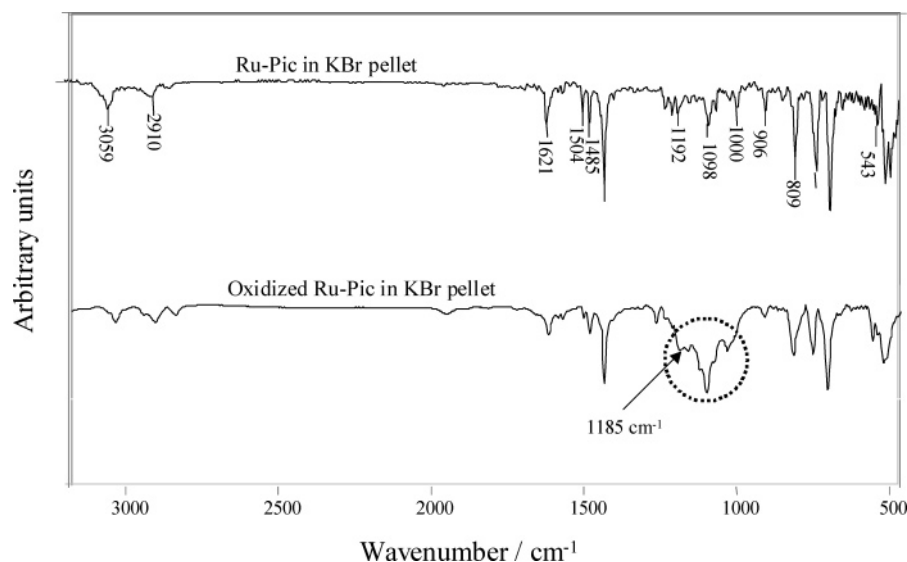


Figure 4. Transmission FTIR spectra for Ru-Pic in a KBr pellet and after oxidation of the phosphine.

of the biphosphine group. Therefore, the color change must be attributed to the oxidation of the phosphorus ligand, which occurs only in the presence of water and air, during the formation of the Langmuir film. This oxidized state remains in the LB film. In complementary experiments, the possibility that the color change could be due to an organic solvent effect was also discarded. In the latter experiments no changes were observed when solutions were prepared with methanol, chloroform, acetonitrile, and propylene carbonate.

Figure 5 shows the fluorescence spectrum for the Ru-Pic complex in the powder form and the surface-enhanced fluorescence (SEF) spectra for cast and LB films, which were deposited onto glass slides coated with 10 nm Ag islands. The emission observed after excitation with the 514.5 nm laser line is practically nonexistent for solution and cast films, while it is much stronger for 1- and 11-layer LB films. Organization in the LB film may impose restrictions to the molecules, which increases emission. For the cast films, relaxation is the dominant process. It should be noted that the 514.5 nm laser line used in the measurements of Figure 5 is in full resonance with the cast

film and in preresonance with the LB films. Therefore, emission should be stronger for cast films if they had the same organization (molecular restrictions) as the LB films.

Figure 6 shows the transmission FTIR spectra for Ru-Pic in a KBr pellet and for a 61-layer LB film on Si and the RAIRS of a 61-layer LB film deposited onto an Ag mirror (100 nm Ag). The assignments for the main peaks measured for the LB film on Si are given in Table 1.^{17,20–23} It should be noted that the “band” at ca. 1800 cm^{-1} for Ru-Pic on Ag mirror is an experimental artifact. The combined use of reflection–absorption and transmission spectra allows one to discuss the molecular orientation in thin films thanks to simple surface selection rules in infrared spectra.^{24,25} The absorption is proportional to the scalar product between the direction of the dynamic dipole (μ') of each normal mode and the direction of the electric field (E) of light at the surface. In the transmission infrared experiment, the electric field lies on the substrate plane, while in RAIRS the main component of E is perpendicular to the substrate surface, as shown in the inset of Figure 6. The differences in the relative intensities using reflection and transmission modes

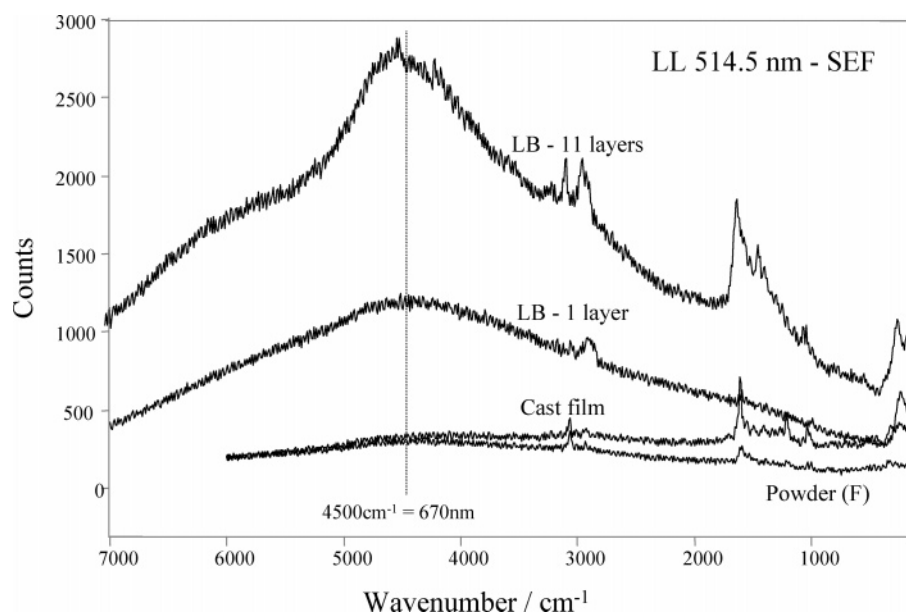


Figure 5. Fluorescence spectrum of a powder Ru-Pic sample and SEF spectra of an 11-layer and a 1-layer LB films and a cast film of Ru-Pic using the 514.5 nm laser line.

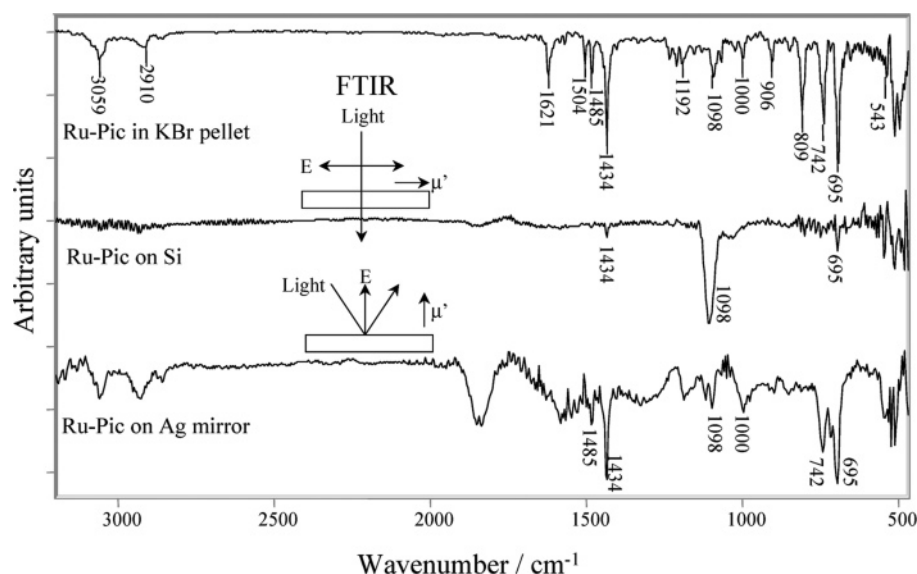


Figure 6. Transmission FTIR spectra for a powder sample and a 61-layer LB film for Ru-Pic on Si and RARS spectrum for a 61-layer LB film on Ag mirror for Ru-Pic. The surface selection rules for transmission and reflection–absorption (RARS) infrared spectroscopy are also indicated.

TABLE 1: Wavenumbers and Assignments^{13–17} for the Main Peaks from the Ru-Pic LB Film on Si

center (cm ⁻¹)	assignments
3059	C–H aryl stretch
2910	C–H alkyl stretch
1485	P–C stretch
1434	P–C stretch or C–H bending
1098	P–C stretch
1000	P–C stretch
906	ring deformation
742	C–H wagging
695	C–H wagging

indicate a preferred molecular orientation in the LB film, as is also suggested by fluorescence spectroscopy (Figure 5). It is observed that for the 61-layer LB film the band at 1098 cm⁻¹ (assigned to the P–C bond in phosphine) dominates the transmission spectrum. The relative intensity of this band is drastically reduced in RARS, which can be explained by assuming that the phosphine groups lie flat on the substrate plane.

Figure 7 shows the Raman scattering (RS) of Ru-Pic powder and the SERS spectra of a cast and an 11-layer LB film on Ag islands (10 nm mass thickness) recorded with the 633 nm laser line. A more crowded spectrum is seen for the LB film compared with that of the thicker cast film. Both spectra have the characteristic C–H stretching modes of the aromatic ring above 3000 cm⁻¹ and the aliphatic C–H stretches below 3000 cm⁻¹. The SERS spectra obtained with a 514.5 nm laser are presented in Figure 8. It should be pointed out that the absolute intensity of the normal Raman of the cast and 11-layer LB films deposited on glass is extremely low. Therefore, the spectrum for the Ru-Pic powder is used as a reference.²⁶ Since the 514.5 and 633 nm laser lines are close to be in resonance with the electronic absorptions seen in Figure 3a, a comparison of the Raman spectra recorded with these two laser lines may provide information about the electronic absorption spectra presented in Figure 3a. The 633 nm laser line is in preresonance with the electronic absorption band at 690 nm for the LB film while the

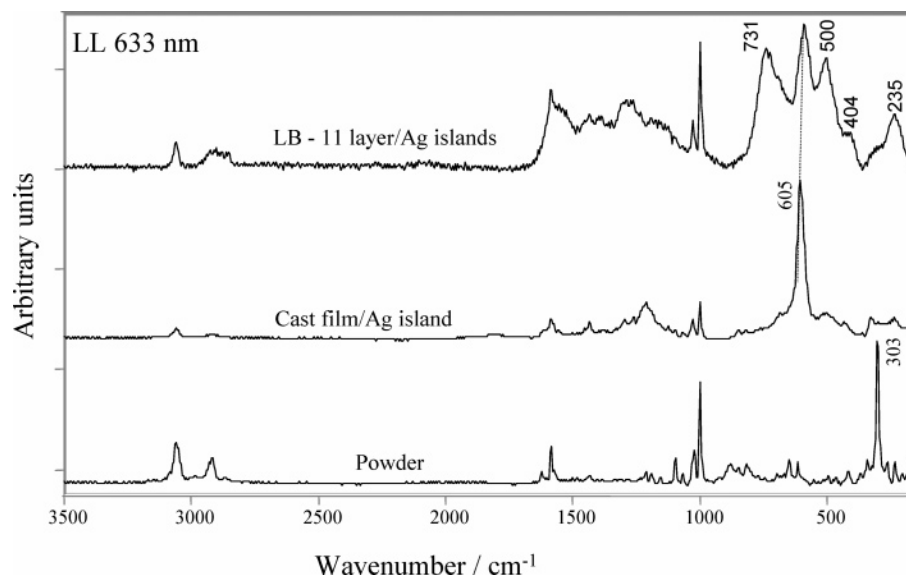


Figure 7. Raman spectra recorded using the laser line at 633 nm for an 11-layer LB film and a cast film on 6 nm Ag islands and for a powder sample of Ru-Pic.

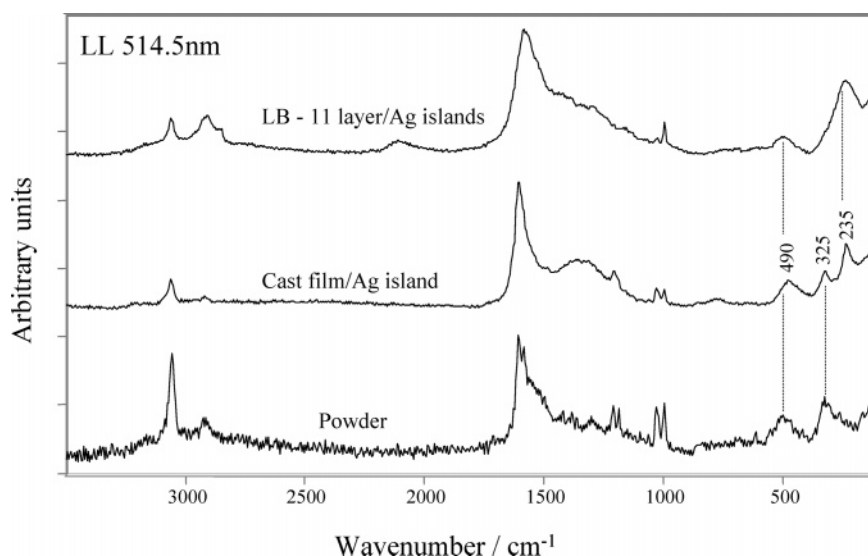


Figure 8. Raman spectra recorded using the laser line at 514.5 nm for an 11-layer LB film and a cast film on 6 nm Ag islands and for a powder sample of Ru-Pic.

514.5 nm laser line is in resonance with the band at 530 nm (see Figure 3a). The main differences between the spectra of LB and cast films are at the region below 800 cm^{-1} where the spectra recorded with the 633 nm laser line for the LB films contain the bands at 731 cm^{-1} attributed to $\gamma(\text{C-H})$, the intense bands at 605 and 500 cm^{-1} assigned to $\nu(\text{P-C})$ and $\nu(\text{Ru-P})$, respectively,²³ and the $\nu(\text{Ru-N})$ band at 404 cm^{-1} .²⁷ The medium-intensity band at 303 cm^{-1} could be assigned to the Ru-Cl antisymmetric stretching.²⁸ Since the P-Ru stretching band at 500 cm^{-1} is seen with a stronger relative intensity in the spectrum recorded with the 633 nm laser line than in spectrum excited with the 514.5 nm line, it seems reasonable to associate the electronic absorption band at 690 nm with the P-Ru moiety (charge-transfer transition).

The question arises as to whether the absorption band at 690 nm for the LB film is caused by a shift in the 530 nm band in the cast film, with the latter being also assigned to P-Ru. If the assumption of a shift is correct, the P-Ru band should also dominate the Raman spectra taken at the 514.5 nm laser line, which is in full resonance with the 530 nm absorption band. However, Figure 8 shows that the band at 500 cm^{-1} is very

weak, hinting that the band at 530 nm in the UV-vis spectra of the cast film (Figure 3a) cannot be assigned to the P-Ru charge transfer. This band cannot be assigned to the Cl-Ru charge-transfer either. The Raman band at 303 cm^{-1} in the powder spectra due to Cl-Ru stretching is much weaker for the 514.5 nm laser line (Figure 8) than for the 633 nm laser line (Figure 7). By exclusion, the absorption band at 530 nm should be attributed either to Ru-N or to benzene rings.²⁹ To distinguish between these two latter possibilities, we consider the spectra of Figure 8 taken with the 514.5 nm laser line. The Raman band at ca. 1600 cm^{-1} associated with benzene rings dominates the spectra for powder, LB, and cast films, from which we can infer that the electronic absorption band at 530 nm is probably related to the benzene rings. It is important to stress that the spectrum of cast films differs from that of the powder for the 633 nm laser line (Figure 7) probably due to an interaction between Ag from the substrate and Cl. This makes the band associated with Ru-Cl practically disappear for the cast film. The band at 235 cm^{-1} seen in Figures 7 and 8 could be an indication of the Ag-Cl interaction for cast and LB films deposited on Ag.

Conclusion

Multilayer LB films of Ru-Pic have been fabricated onto several substrates. The absorption spectrum shows that the same amount of material was deposited in each transfer cycle. Ru-Pic LB films display a characteristic bluish color different from that of the complex in solution or in cast films. This peculiar absorption spectrum is associated with the oxidation of the phosphine moieties. Therefore, the absorption band at 690 nm, which is responsible for the distinct color of the LB films, is not due to a shift in the 530 nm band observed for Ru-Pic in the other forms (powder, solution, and cast films). Organization and molecular orientation in the LB films were confirmed by fluorescence emission spectroscopy and extracted from the complementary information provided by transmission and reflection-absorption infrared spectra. Using surface-enhanced Raman spectroscopy with two laser lines, in resonance or preresonance with the absorption bands at 530 or 690 nm, a selective enhancement of the vibrational bands of the corresponding functional groups permitted the identification P–Ru charge transfer as the 690 nm band. The band at 530 nm is associated with the aromatic groups.

Acknowledgment. Financial assistance from FAPESP, CNPq, and Fundação Araucária (Brazil) and NSERC (Canada) is gratefully acknowledged. The authors are also indebted to Dr. Mauro Fernandes (IQSC/USP) for the use of FTIR Bomem MB 102 and Hitachi U-3000 UV–vis equipment.

References and Notes

- (1) Ferreira, M.; Wohnrath, K.; Torresi, R. M.; Constantino, C. J. L.; Aroca, R. F.; Oliveira, Jr., O. N.; Giacometti, J. A. *Langmuir* **2002**, *18*, 540.
- (2) Wohnrath, K.; Garcia, J. R.; Nart, F. C.; Batista, A. A.; Oliveira, Jr., O. N. *Thin Solid Films* **2002**, *402*, 272.
- (3) Töllner, K.; Ronit, P.-B.; Lahav, M.; Milstein, D. *Science* **1997**, *278*, 2100.
- (4) Abatti, D.; Zaniquelli, M. E.; Iamamoto, Y.; Ydemori, Y. M. *Thin Solid Films* **1997**, *310*, 296.
- (5) Riul, Jr., A.; Santos, D. S.; Wohnrath, K.; Di Thommazo, R.; Carvalho, A. A. C. P. L. F.; Fonseca, F. J.; Oliveira, Jr., O. N.; Taylor, D. M.; Mattoso, L. H. C. *Langmuir* **2002**, *18*, 239.
- (6) Zhang, C. R.; Yang, K. Z.; Jin, W. R. *Thin Solid Films* **1996**, *285*, 533.
- (7) Santos, J. P.; Batalini, C.; Zaniquelli, M. E.; De Giovanni, W. F. *XI Simpósio Brasileiro de Brasileiro de Eletroquímica e Eletroanalítica*; Gramado: Brasil, 1999.
- (8) Santos, J. P.; Zaniquelli, M. E.; Batalini, C.; De Giovanni, W. F. *J. Phys. Chem. B* **2001**, *105*, 1780.
- (9) Delavie, P.; Lee, J. R.; Sprintschnik, H. W. *J. Am. Chem. Soc.* **1977**, *99*, 7094.
- (10) Daifuku, H.; Aoki, K.; Tokuda, K.; Matsuda, H. *J. Electroanal. Chem.* **1985**, *183*, 1.
- (11) Fu, Y.; Ouyang, J.; Lever, A. B. P. *J. Phys. Chem.* **1993**, *97*, 13753.
- (12) Murakata, T.; Miyashita, T.; Matsuda, M. *J. Phys. Chem.* **1988**, *92*, 6040.
- (13) Santos, J. P.; Zaniquelli, M. E.; Batalani, C.; De Giovanni, W. F. *Thin Solid Films* **1999**, *349*, 238.
- (14) Tamura, K.; Sato, H.; Yamashita, S.; Yamagishi, A.; Yamada, H. *J. Phys. Chem. B* **2004**, *108*, 8287.
- (15) Wohnrath, K.; Araújo, M. P.; Batista, A. A.; Dinelli, L. R.; Oliva, G.; Castellano, E. E.; Ellena, J. J. *Chem. Soc., Dalton Trans.* **2000**, *19*, 3383.
- (16) Dhanabalan, A.; Balogh, D. T.; Riul, Jr., A.; Giacometti, J. A.; Oliveira, Jr., O. N. *Thin Solid Films* **1998**, *323*, 257.
- (17) Duff, C. M.; Heath, G. A. *J. Chem. Soc., Dalton Trans.* **1991**, *9*, 2041.
- (18) Wohnrath, K.; Mello, S. V.; Pereira-da-Silva, M.; Oliveira, Jr., O. N. *Synth. Met.* **2001**, *21*, 425.
- (19) Nakamoto, K. *Infrared and Raman Spectra of Inorganic and Coordination Compounds*, 3rd ed.; Wiley: New York, 1978; p 226.
- (20) Sheldrick, W. S.; Brandt, K. *Inorg. Chim. Acta* **1994**, *217*, 51.
- (21) Daasch, L. W.; Smith, D. C. *Anal. Chem.* **1951**, *23*, 853.
- (22) Silverstein, R. M.; Bassler, G. C.; Morrill, T. C. *Spectrometric Identification of Organic Compounds*, 5th ed.; John Wiley & Sons: New York, 1991; Chapter 1.
- (23) Khan, M. M. T.; Reddy, V. J. *Coord. Chem.* **1982**, *12*, 71.
- (24) Debe, M. K. *Prog. Surf. Sci.* **1987**, *24*, 1.
- (25) Greenler, R. G. *J. Chem. Phys.* **1966**, *44*, 310.
- (26) Moscovits, M. *Rev. Mod. Phys.* **1985**, *57*, 783.
- (27) Alessio, E.; Balducci, G.; Lutman, A. *Inorg. Chim. Acta* **1993**, *203*, 205.
- (28) Albinati, A.; Jiang, Q.; Rüegger, H.; Venanzi, L. M. *Inorg. Chem.* **1993**, *32*, 4940.
- (29) Antunes, P. A.; Constantino, C. J. L.; Aroca, R. F. *Langmuir* **2001**, *17*, 2958.